Coupling a distiller and an electrochemical cell for energy production from low temperature heat sources.

A. Carati M. Marino D. Brogioli*

15 Aprile 2015

Abstract

We aim at exploiting the heat sources at very low temperature, below 150° (e.g. low-concentration solar and industrial waste heat) for production of electrical energy, in particular for small power applications. In this case, traditional techniques, such as organic Rankine cycle, Stirling engines and solid-state devices based on Seebeck effect, are not economically viable. We explore a low-cost, easily down-scalable electrochemical method working with a closed cycle: a salinity-gradient-power device produces electrical current by consuming the concentration difference between two solutions; the mixed solutions it produces are sent to a distiller which restores the concentration difference, in turn exploiting the low-temperature heat source. The "battery mixing", a newly introduced salinity-gradient-power technique, enables the exploitation of a wide range of solutes and solvents. In this manuscript, we theoretically analyse the whole cycle, in order to enable an educated choice of solutes and solvents with respect to the efficiency in the conversion of heat into electrical power. We find that the main requirement is a high boiling point elevation; minor advantages are obtained by solutions with a high latent heat of vaporisation and low specific heat capacity. The first two requirements could appear counter-intuitive, since they are detrimental in the case of distillation processes *per se*. Quite surprisingly, the electrochemical parameters play a minor role in determining the efficiency. Our results allow to devise solutions for single-effect processes that give a high efficiency, close to the Carnot limit, for very low temperature heat sources (e.g. 11% for a temperature difference of 40 K), competitive with the more traditional techniques but much cheaper and easily down-scalable.

*Università degli Studi di Milano, Dipartimento di Matematica, via Saldini 50, 20133 Milano (Italy). E-Mail:dbrogioli@gmail.com

1 Introduction

The free energy contained in solutions with different concentrations can be tapped and converted into electrical energy by means of the so-called "salinity gradient power" (SGP) techniques, e.g. by means of a concentration-difference electrochemical cell [7].

Various SGP techniques have been proposed for the conversion of the concentration differences into current. They were often conceived as a mean for the production of completely clean and renewable energy by exploiting the naturally occurring solutions with different concentrations [24, 21, 15]. Such solutions include river and sea waters, and brines from salt lakes (e.g. Dead Sea) [14], from coal-mines (produced by dissolving geological deposits) [34], and from salterns [6].

Recently, various researchers proposed to apply instead these techniques in situation in which the difference in concentration is produced by means of distillation [13, 18]. In other terms, these authors proposed to use the following thermodynamical cycle: the solutions with different concentrations enter into the SGP cell, which exploits part of the available mixing free energy. The outgoing solutions are then completely mixed and are sent to a distiller, where the concentration difference is restored so that a new cycle can take place. The whole device, which operates in closed-cycle with respect to the involved masses, can be considered as a heat-to-current converter (HTCC), conceived for exploiting low-temperature heat sources.

In the literature, a thermodynamical analysis of such a cycle is apparently lacking. The present work aims at finding how the efficiency of the HTCC depends on the thermo-physical parameters of the solutions, allowing for a selection of the solutions that gives a high efficiency η, namely the ratio between the produced electrical work and the heat adsorbed from the heat source.

It will be shown in Sect. "Thermodynamical efficiency of the distiller stage" that the efficiency improves as the boiling point of the more concentrated solution increases. A weaker improvement is obtained by using a solvent with a high latent heat of vaporisation and with a low specific heat capacity. Such parameters will constitute clues for the selection of candidate solutions to be used in our HTCC. Using solutions of a strong electrolyte in water an efficiency can be reached close to that of a Carnot cycle working between the boiling point of the more concentrated solution and the boiling point of the pure solvent.

It is worth noting that the role of the first two parameters (i.e. boiling point elevation and latent heat of vaporisation) could be counter-intuitive,

since they have a detrimental effect in distillation. The question can be settled by remarking that our aim of increasing the free energy content of the solution is different from that of distillation, that aims at the maximum production of concentrated solution or distillate.

Now, as a matter of fact, the overall efficiency η is the product of the efficiencies of the distiller stage and of the SGP cell:

$$\eta = \eta_{dist}\eta_{SGP}, \tag{1}$$

where η_{dist} is the efficiency of the distiller in converting heat into the mixing free energy of the solutions and η_{SGP} is the efficiency of the SGP device in converting the free energy into electrical energy. At any rate, the overall heat to current conversion performance is dependent essentially on the thermo-physical properties of the solutions, relevant for the operation of the distiller stage. The analysis performed in Sect. "Thermodynamical efficiency of the distiller stage" will show that it is possible to give a rough evaluation of the efficiency of the HTCC only in terms on the thermo-physical parameters of the solutions, relevant for the distiller stage, because such thermo-physical parameters also determine the power output and the voltage (or voltage rise) of the SGP cell.

In this paper, we will consider an SGP device based on electrochemical principles of operation, so that the HTCC we study falls in the broader category of the "thermally regenerated electrochemical cells" [28], in which the regeneration takes place by means of a thermal effect (either physical, such as distillation, or chemical) and the electrochemical cell exploits a composition difference between solutions. Some examples are given by copper redox flow battery [25] or cells based on complexation of copper ions by ammonia [36]. In various patents (e.g. WO 2012012767 and US 4292378), the electrochemical SGP devices is based on reverse electrodialysis (RED) [35, 26, 27], in which the feed solutions are sent through a stack of ion-exchange membranes; the ion diffusion which takes place across the membranes constitutes a current that can be extracted from the cell. Although all the cited techniques allow, at least in principle, to reach a high efficiency η_{SGP} of the electrochemical SGP device (50%-80%), the overall efficiency η is much lower, due to the low efficiency of the distiller stage; up to now, this obstacle has not been recognised in literature as the most limiting element of the technique.

A novel family of SGP techniques has been recently introduced for the exploitation of naturally occurring salinity differences: it includes the "capacitive mixing" (CapMix) [2, 31, 3, 5, 1, 29, 4] and "mixing entropy battery" or "battery mixing" (BattMix) [13, 10]. The latter technique can be efficiently applied also to the artificially produced solutions used in the HTCC;

indeed, BattMix devices specifically designed for lithium chloride and zinc chloride solutions have been studied [2, 13, 17, 16].

The BattMix technology allows to reach higher overall efficiencies. The reason resides in the possibility of exploiting unusual and much more concentrated solutions with respect to the membrane-based RED technique; this allows to reach a higher efficiency η_{dist} of the distiller stage. For example, we will show that a HTCC cycle working with a BattMix cell using aqueous zinc chloride solutions can theoretically reach an efficiency of 8% with the very small temperature difference of 40 K [17] (see Sect. "Nominal power and efficiency"). The performances of the SGP cells, with RED and BattMix technologies, are described in Sect. "Power output and efficiency of the electrochemical cell". There, it will be shown that various SGP technologies could attain a good efficiency η_{SGP} (up to 80%) in the conversion of the free energy of the feed solutions into electrical energy, making our approach feasible.

We now make a comparison between our approach for the heat-to-current conversion and the more traditional ones. We recall that the conversion of heat to mechanical work is traditionally obtained by means of heat engines (see for example [33]), and in the cases of low temperature sources the Stirling motors or organic Rankine cycle devices are proposed. However, the quest for alternative methods, less relying on moving parts, is an important research field.

The HTCC we propose has several advantages over the traditional solutions. First of all, thanks to the limited presence of moving parts, the devices need a very limited amount of maintenance, making them suited for domestic and small-scale applications. Another remarkable advantage of this scheme is that it can produce electric power on demand, because the solutions produced by the distiller during a few hours (e.g., around noon for solar energy) can be stored and used later, when needed, by the SGP cell. For example, the SGP cell can work at a lower power rate and provide a continuous supply of electric power. The decoupling of the source from the load is usually a big problem with the actual use of renewable energy, and it is usually implemented by means of batteries or redox flow batteries, which *vice versa*, in our scheme, are the main supplies of electric power (and not an additional accessory). So, with our HTCC scheme, this important feature is easily obtained by the inexpensive storage of liquids.

The required heat can be easily obtained by a renewable source as the solar energy. In Sect. "Example of realization of the process" we present a practical scheme of a single-effect device, working in a continuous regime. Due to the small needed temperature difference (of the order of 40 K for

zinc chloride solutions), the device can be put in operation by using the heat from solar radiation, without the need for concentration. By using solutions with a higher boiling point elevation, such as sulfuric acid in water, we can exploit a larger temperature difference, leading to a better efficiency. Such a larger temperature differece can be provided by low levels of solar concentration, wich can be inexpensively achieved [11] by means of the concentrators working with the so-called non-imaging optics [20, 32]. Such solar concentrators, not requiring tracking, are suited for domestic applications, and, by using selective absorbers, the heat collectors can work with good efficiency also at a not so low temperature, for example 50% at 180°C. Our HTCC can be efficiently used also in other applications besides the solar energy field, which include co-generation [22, 30, 23] and recovery of waste heat from industrial processes, contributing to the renewable and clean energy production.

Finally, we want to stress that our overall analysis of the HTCC can be applied not only to distillation, but to any method based on the coexistence of a liquid phase (solution) and a vapour phase in equilibrium, such that the composition of the liquid phase depends on temperature.

2 Power output and efficiency of the electrochemical cell

2.1 Nominal power and efficiency

The parameters of the SGP devices that are often reported are the power (per electrode surface or volume) and the efficiency, namely the ratio between the produced energy and the available mixing free energy ΔG of the incoming solutions. Both quantities usually represent the "nominal" values, P_{nom} and η_{nom}, obtained in somehow optimal conditions. For example, the power P_{nom} is evaluated at the optimal impedance coupling, while the efficiency η_{nom} is obtained at low current. The two nominal performances cannot be obtained together with the same operational parameters; a trade-off between the optimisation of them must be found (see next section).

The RED technique is often applied to sea-river water feed solutions; in this case, the cell nominal power P_{nom} if of the order of 0.1-1 W/m^2, mainly depending on the membrane performances [26], while a few W per square meter can be reached with NaCl brines. The CapMix technique currently reaches 30 mW/m^2 with activated carbon electrodes in sea-river water, and does not increase its performances when brines are used. The

BattMix technique reaches a power of approximately 100 mW/m^2, which can be increased with the use of brines. The use of solutions, other than NaCl, allow to increase the power output of BattMix techniques. With zinc chloride and zinc electrodes, the power of 3 W/m^2 has been reached in proof-of-principle cells [17, 16]. An interesting thermally regenerative battery [25], based on Cu^+ ions, reaches a power that can be evaluated around 20 W/m^2.

For what concerns the nominal efficiency η_{nom}, notwithstanding it does not include the detrimental effects of the overvoltage (being measured to very low output power), however, one has always $\eta_{nom} < 1$, because the cell voltage does not match the difference of the chemical potential of the solute between the concentrated and diluted solution. This happens for many reasons, including parasitic reactions involving ions other than the solute, unwanted mixing in the cell, leakage currents.

In the case of sea-river water, an efficiency more than 80% can be achieved with RED [26]. Instead, the membranes used in RED do not perform that well at the high concentrations needed in order to have a good thermodynamicall efficiency of the distillation stage (see below). In fact the actual voltage ΔV_{eff} of the RED cell will be decreased with respect to its "ideal" behaviour, by increasing the concentration above a certain threshold. The voltage ΔV_{eff} depends actually by the mean mole fraction $\bar{c}$ of the active groups of the ion exchange membranes, as shown in [27]. Under the simplifying hypothesis of ideal solutions, for $c_H \gg \bar{c}$, the voltage ΔV_{eff} is given by

$$\Delta V_{eff} \approx \frac{2K_BT}{ze} \log\left(\frac{\bar{c} + \sqrt{4c_L^2 + \bar{c}^2}}{2c_L}\right) < \frac{2K_BT}{ze} \log\left(\frac{\bar{c}}{c_L} + 1\right) \qquad (2)$$

The membranes have usually $\bar{c}$ of the order of 3 M, far less than c_H we aim to use, so that this result can be roughly interpreted by saying that a RED device would exploit a concentration difference between c_L and $\bar{c}$, instead of the much higher difference between c_L and c_H.

Limitation of such a type do not apply to other techniques. For example with the CapMix technique, good efficiency was obtained in the case of zinc chloride solutions [17] and lithium chloride solutions [13]. Also batteries batteries have a relatively high energy efficiency: the nominal efficiency η_{nom} is of the order of 70-90% in the case of the above-mentioned thermally regenerative battery [25], while for other type one has from literature 80% for zinc–bromide , 66–72% for Fe-Cr, 72% for all-vanadium, and 70-74% for lead-acid batteries [8].

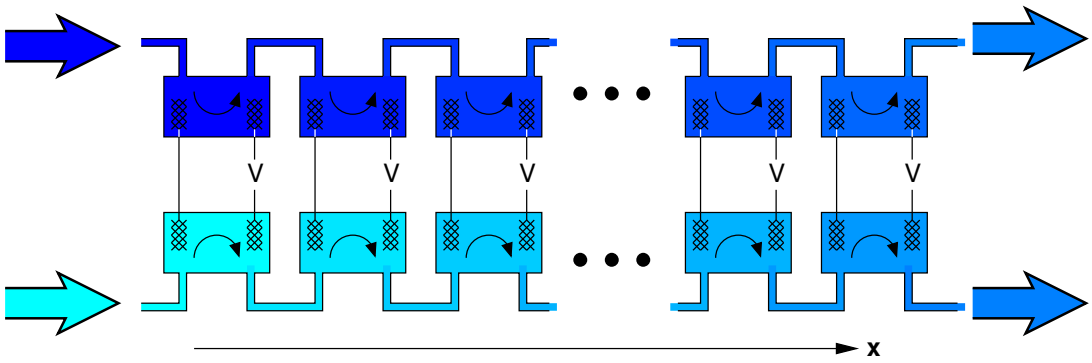

Figure 1: Sequence of cells that work at different concentrations, consuming the concentration difference.

In the next section we'll examine the behaviour of η as a function of the actual output power of a cell.

2.2 Operation for complete consumption of the mixing free energy

The parameters P_{nom} and η_{nom} defined in the previous section refer to particular operating conditions, in particular, to a particular (optimal) value of the concentrations and of the currents. In real operations, the solution concentration will change, because the solution concentration difference is slowly exploited for producing energy; moreover, the current must be selected with a trade-off between power production and efficiency. In this section, we evaluate the average power output and the efficiency over the whole process, starting with given solutions and ending with the solutions completely mixed, provided that the process is performed under optimal conditions. The goal is to exploit, as much as possible, the available mixing free energy of the solutions; for an example of this in the case of RED, see Ref. [12].

We parametrise the process with a "mixing parameter" x, which takes a value 0 when the initial solutions are not mixed and 1 when the solutions are completely mixed by the action of the SGP device. We assume that the SGP operation starts at $x_0 > 0$, i.e. with partially mixed solutions, for avoiding the high resistance of the pure solvent, and it ends at $x_1 < 1$, i.e. with not completely mixed solutions, since the cell voltage vanishes for $x \to 1$. The parameter x can be interpreted as representing the time in a batch process, or as a spatial coordinate, as in Fig. 1.

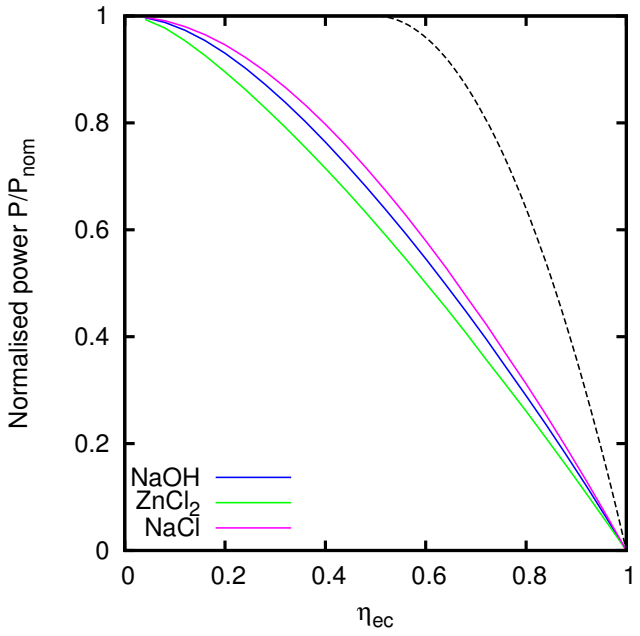

Figure 2: Dependence of the maximum produced power P on the energy efficiency η_{SGP} of the electrochemical cell. The points have been obtained for an AccMix cell working with $ZnCl_2$ solutions [17] at molar fractions of c_L=0.01 and c_H=0.1 and a cell working with NaOH solutions at molar fractions c_L=0.03 and c_H=0.3 (see Supporting Information, Sect. 2 for the details of the calculation). The dotted line represents an ideal situation in which the voltage does not depend on the concentration.

The parameters that we choose to optimise are x_0, x_1 and the current $I(x)$ (this last parameter is a function of x). In order to discuss the trade-off between P and η_{SGP}, we find the maximum of P as a function of x_0, x_1 and $I(x)$, with a fixed value of η_{SGP} in the range between 0 and 1. The calculation is reported in SI Sect. 1 and 2.

Figure 2 shows the dependence of P on η_{SGP}, calculated for various solutions. We assume that the overvoltage is linear in the current, so that the "nominal power" of the cell is $P_{nom} = 1/4V_0^2/R_0$, where V_0 and R_0 are the cell voltage and resistance in the conditions under which the nominal power is evaluated. In the graph, the power is normalised with respect to the nominal power. The graph also reports the particular case of constant

voltage, in which the optimisation can be easily done analitically. In that case, we can recover the traditional result that, at the optimal impedance matching, at which P_{nom} is evaluated, the energy efficiency is 1/2.

From Fig. 2 we conclude that a quite high efficiency η_{SGP} can be obtained, with a trade-off with the power. For example, if a given device, with a given volume, has a nominal power P_{nom}, for obtaining an efficiency of 80% and a power $P = P_{nom}$, the volume of the device must be multiplied by a factor approximately 4.5.

3 Thermodynamical efficiency of the distiller stage

In this section we discuss the efficiency η_{dist} of the distiller stage:

$$\eta_{dist} = \frac{\Delta G}{Q_H}, \tag{3}$$

where ΔG is the available mixing free energy of the solutions produced by the distiller and Q_H is the heat that the system adsorbs from the heat source. In turn:

$$\Delta G = G\left(n_s, n_w\right) + G\left(0, n'_w\right) - G\left(n_s, n_w + n'_w\right), \tag{4}$$

where $G\left(n_s, n_w\right)$ is the Gibbs free energy of a solution with n_s moles of solute and n_w moles of solvent. In this section, we also assume that the electrochemical cell is ideal, i.e. that it produces a work $W = \Delta G$.

We focus on a batch operation performed by the cycle described in Fig. 3. All the process takes place at a constant pressure P. We assume that the every phase of the cycle is long enough for reaching a complete temperature equilibration. The cycle starts with the compartments of the concentration difference cell filled with a solution S_0 at concentration c_0 and with an amount of distilled solvent W_0 respectively. The boiling point of the solution S_0 and of the pure solvent W_0 are respectively T_H and T_L. The cycle is composed of the following five phases:

I. The electrochemical cell operates at temperature T_L, reversibly, until it is completely discharged, i.e. the solutions in the two compartments reach the same concentration c_1.

II. The total amount of solution S_1 at concentration c_1 is heated from T_L to T_1, the boiling point of the solution.

III. An amount of solvent equal to W_0 is evaporated from the solution S_1; the temperature increases from T_1 to T_H.

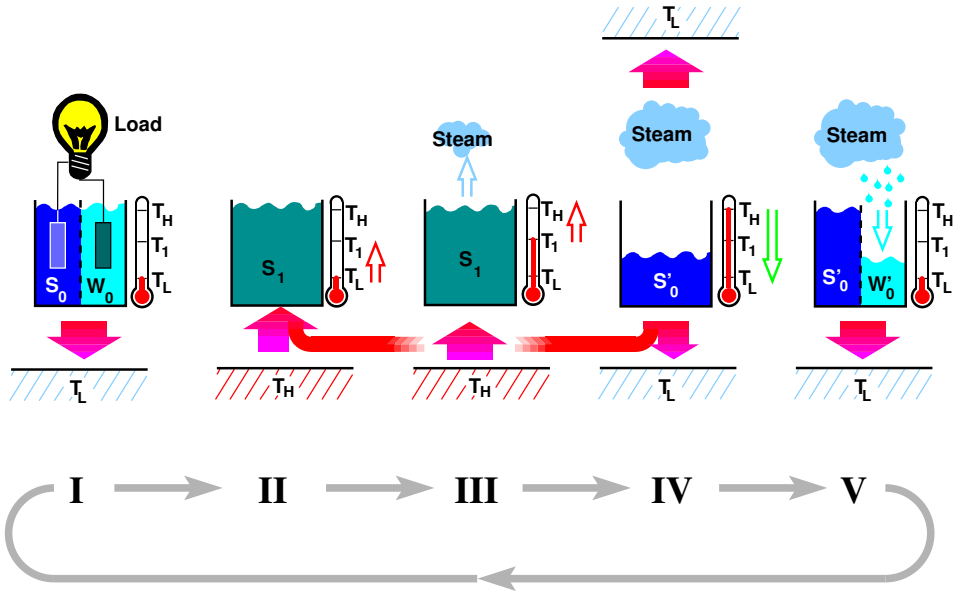

Figure 3: Ideal implementation of the HTCC with batch operation with complete equilibration at the end of each phase. In phases II and IV the system adsorbs heat from the heat source at T_H while in the other phases it is in contact with the heat sink at T_L. A partial heat recovery, without heat exchages with the source and sink, takes place between phases II and IV.

IV. Both the evaporated solvent and the remaining solution S_0' are cooled from T_H to T_L. The solution S_0' goes into the high-concentration compartment of the cell.

V. The solvent vapor is condensed at temperature T_L. The resulting solvent W_0' goes into the low-concentration compartment of the cell.

The heat is exchanged between the system and the heat source and sink, respectively at temperature T_H and T_L. We immediately see that the efficiency η_{dist} is less than η_C:

$$\eta_C = \frac{T_H - T_L}{T_H}, \tag{5}$$

i.e. the efficiency of a Carnot cycle operating between T_H and T_L. Irreversible heat exchanges take place in phases II, III and IV, because of an abrupt contact between the cell with the heat source and sink at a different temperature, and thus the efficiency η_{dist} is strictly less than η_C; however, we will see that it is indeed possible to get close to this limit, i.e. to operate the HTCC not too far from reversibility. It is worth noting that η_C is of the order of 10%, e.g. for $ZnCl_2$ solutions, for a temperature difference of 40 K, but could be of the order of 20-25%, e.g. with sulfuric acid solutions.

Under the very rough assumption that the main heat consumption is needed for the evaporation of water, Q_{evap}, and that the cycle has an efficiency η_C, we get $W \approx Q_{evap}\eta_C$. We thus see the importance of having a high boiling point elevation and a high latent heat of vaporisation: the more heat we need in vaporisation the more work we produce. This is somewhat counterintuiteve, since both features are retrimental in distillation.

It can be noticed that the heat released by the system in phase IV is at higher themperature than the heat provided to the system in phase II. Thus we consider the possibility of providing a fraction α of heat needed in phase II by recoverying heat pf phase IV. This will help to increase the efficiency. It is worth noting that this heat recovery does not involve the latent heat.

The discussion above highlights the importance of the boiling point elevation. In Fig. 4 we show the boiling temperature at pressure P=1 atm of solutions of various solutes, as a function of the concentration. We can see that the various solutes give a different boiling point elevation, which increases with the concentration; the maximum boiling point elevation that can be achieved with a given solute is limited by its maximum concentration. For NaCl and NaOH the maximum concentration is chosen in order to avoid crystallisation at room temperature; for $ZnCl_2$, the concentration is limited by the increase of viscosity.

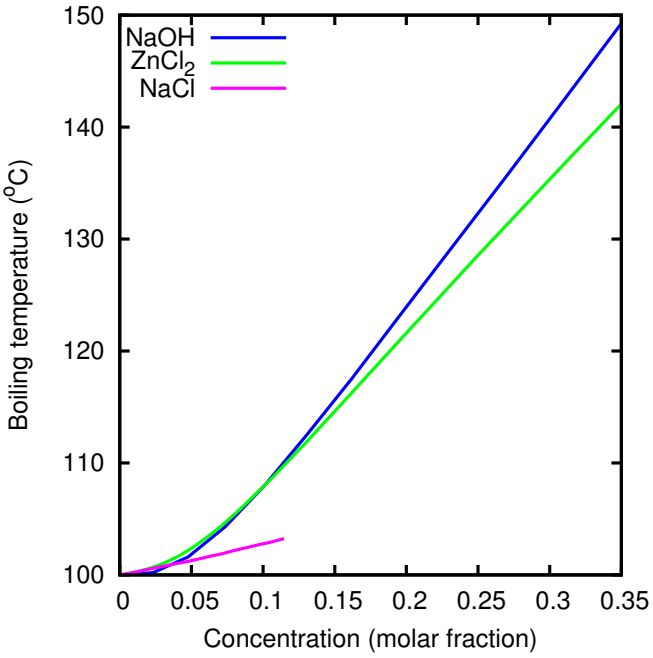

Figure 4: Boiling temperature at atmospheric pressure of aqueous solutions of NaOH, $ZnCl_2$ and NaCl. The data for the NaCl stop at the molar fraction corresponding to the solubility of the salt.

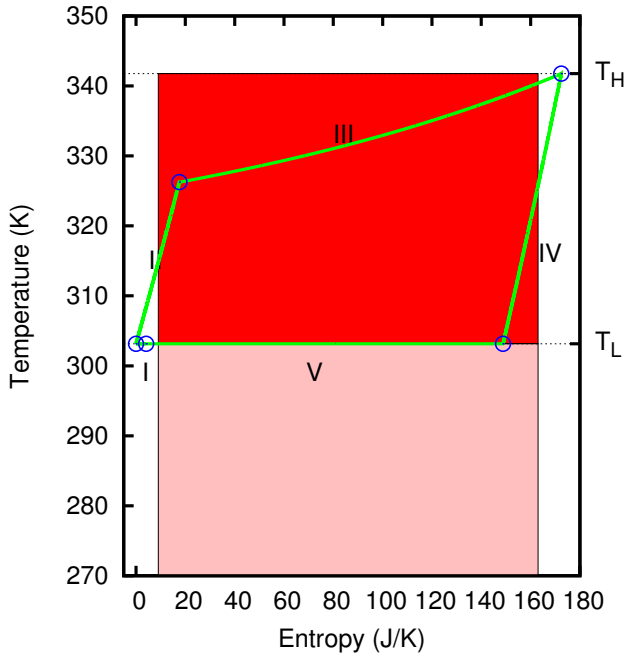

Figure 5: Cycle in the T vs. S plane. The red and pink areas represent the produced work and consumed heat in the case of the Carnot cycle.

The distiller will work at a pressure well below P=1 atm, in order to roughly match the condensation temperature of the solvent with the room temperature, assumed to be the heat sink. The precise dependence of the efficiency η_{dist} on the working pressure P will not be discussed here; however, it is worth mentioning that the calculations show that η_{dist} is largely independent on P; a strict independence could be deduced from the so-called "Dühring's rule" [19], which roughly holds in the cases under study.

Now we perform the calculation of the efficiency. Let M be the number of moles of the solution S_0 — defined as the sum of the numbers of moles of solvent and of solute — and m the number of moles of the pure solvent W_0. We define $T_{bp}(c)$ the boiling point of the solution at concentration c and we remind that $T_L = T_{bp}(0)$, $T_1 = T_{bp}(c_1)$ and $T_H = T_{bp}(c_0)$. The concentrations c_0 and c_1 are expressed as molar fractions, i.e. the ratio between the moles of the solute on the one hand and the sum of the moles of the solute and the solvent on the other.

We define $Q_I, \ldots, Q_V$ as the heat absorbed by the cell in phases I, ...,

V; as usual, we attribute a positive sign to the heat absorbed by the system. We can calculate four of them from the thermo-physical parameters, namely:

$$\begin{aligned} Q_{II} &= C(c_1)(M+m)(T_1-T_L) \\ Q_{III} &= \int_{c_1}^{c_0} \left\{ \frac{\lambda(c)}{c} + \left[C(c) + C_s \left(\frac{c_0}{c} \frac{M+m}{M} - 1 \right) \right] \frac{\partial T_{bp}(c)}{\partial c} \right\} M \frac{c_0}{c} \mathrm{d}c \\ Q_{IV} &= -\left[C(c_0) M + C_s m \right] (T_H - T_L) \\ Q_V &= -\lambda(0) m, \end{aligned} \tag{6}$$

where $C(c)$ is the molar specific heat at constant pressure of the solution at concentration c, C_s is the molar specific heat at constant pressure of the solvent vapour (steam), $\lambda(c)$ is the molar latent heat of evaporation of the solution at concentration c at its boiling point. Here we neglect the dependence of the specific heats on temperature. It's worth noting that $\lambda(c)$ can be calculated based on the boiling point elevation, see SI Sect. 4.

Then we define $\Delta S_I, \ldots, \Delta S_V$ as the entropy changes underwent by the cell in phases I, ..., V; we calculate four of them from the thermo-physical parameters:

$$\begin{aligned} \Delta S_{II} &= C(c_1)(M+m) \ln \frac{T_1}{T_L} \\ \Delta S_{III} &= \int_{c_1}^{c_0} \left\{ \frac{\lambda(c)}{c} + \left[C(c) + C_s \left(\frac{c_0}{c} \frac{M+m}{M} - 1 \right) \right] \frac{\partial T_{bp}(c)}{\partial c} \right\} M \frac{c_0}{c T_{bp}(c)} \mathrm{d}c \\ \Delta S_{IV} &= -\left[C(c_0) M + C_s m \right] \ln \frac{T_H}{T_L} \\ \Delta S_V &= -\frac{\lambda(0) m}{T_L}. \end{aligned} \tag{7}$$

Finally we calculate $W = \Delta G$ as:

$$W = \Delta G = Q_{II} + Q_{III} + Q_{IV} + Q_V - T_L (\Delta S_{II} + \Delta S_{III} + \Delta S_{IV} + \Delta S_V), \tag{8}$$

which relies on the hypothesis that phase I is performed isothermally and that the whole cycle is isobaric (see SI Sect. 3).

We define Q_H and Q_L as the heat exchanged respectively with the heat source and the heat sink at T_H and T_L. We assume that a fraction α of the heat released by the system in phase IV is recovered and used for heating the solution in phase II (it must be noted that, in the situations under consideration, $Q_{II} < Q_{IV}$).

$$\begin{aligned} Q_H &= (1-\alpha) Q_{II} + Q_{III} \\ Q_L &= Q_I + \alpha Q_{II} + Q_{IV} + Q_V \end{aligned} \tag{9}$$

This allows us to calculate the efficiency as:

$$\eta = \frac{W}{Q_H} = \frac{Q_H + Q_L}{Q_H}. \tag{10}$$

We see that the produced work (or better the produced free energy of the solutions) and the efficiency can be calculated from the boiling point, the molar specific heat of the solution and the latent heat of vaporisation. It could be surprising that the calculation of the produced work and of the efficiency does not involve the electrochemical parameters of the cell, but this is simply a consequence of the first and the second principles of thermodynamics.

The result of the calculation of the efficiency as a function of temperature T_H of the heat source is shown in Fig. 6. For each point of the graph, the concentration c_0 is chosen so that its boiling point is T_H; if this boiling temperature cannot be reached by that given solution, the concentration c_0 is fixed at the maximum value (see dotted lines in the graph). We see that, with the parameters used in this calculation, the efficiency η_{dist} increases in the same way of η_C; however, when the maximum concentration is reached, the efficiency does not increase any more. This is due to the irreversibility introduced by the fact of having the heat source at a temperature T_H, in contact with the solution at a temperature $T_{bp}(c_{max}) < T_H$. This highlights again the importance of solutions with a high boiling point elevation and a high concentration.

We start now an analysis aimed at understanding the influence of the various parameters on the efficiency. We notice that a rough approximated expression for η_{dist} can be obtained by assuming that: i) the only heat exchanges are the ones for vaporisation and condensation; ii) C and λ are constant; iii) $T_{bp}(c)$ is linear in c; iv) $T_H - T_L \ll T_L$. In this approximation, $Q_{II} + Q_{III} + Q_{IV} + Q_V = 0$, so that the whole mixing free energy has entropic origin; moreover, the recovery ratio α has no effect. We obtain the approximate value η_S:

$$\eta_S = \eta_C f_S\left(\frac{MT_H}{mT_L}\right), \tag{11}$$

where $f_S(x) = x * \log(1 + 1/x)$ is a function which increases monotonically from 0 to 1; for $T_H/T_L \approx 1$ and $M = m$, $f_S(x)$=69%.

The approximation η_S is also shown in Fig. 6 as a dotted black line. We see that it is a better approximation than η_C: indeed, η_S takes into account the irreversible heat exchange taking place at the beginning of the phase III, when the concentration is $c_1 < c_0$ and thus the temperature of the solution is less than T_H, and is brought into contact with the heat source at T_H.

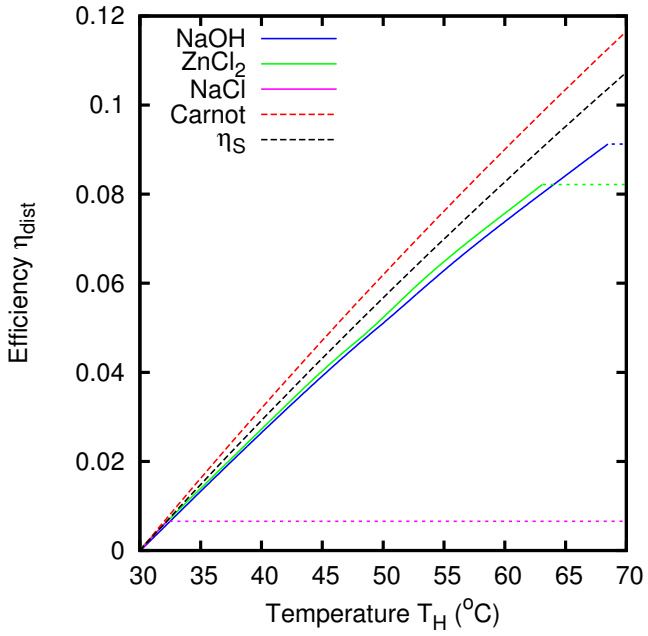

Figure 6: Efficiency of the distiller stage as a function of the temperature T_H of the heat source. The heat sink is at T_L=30°C. The pressure and the molar fraction of the concentrated solutions S_0 (see Fig. 3) are chosen so that the boiling temperature of the pure water and of the concentrated solution are respectively T_L and T_H, with the limit of c_0¡0.34 for the solutions of NaOH and $ZnCl_2$, and c_0¡0.1 for NaCl. The two sets of curves have been obtained with a recovery factor α=80%. The ratio between the moles of produced solution and distilled water is M/m=5.

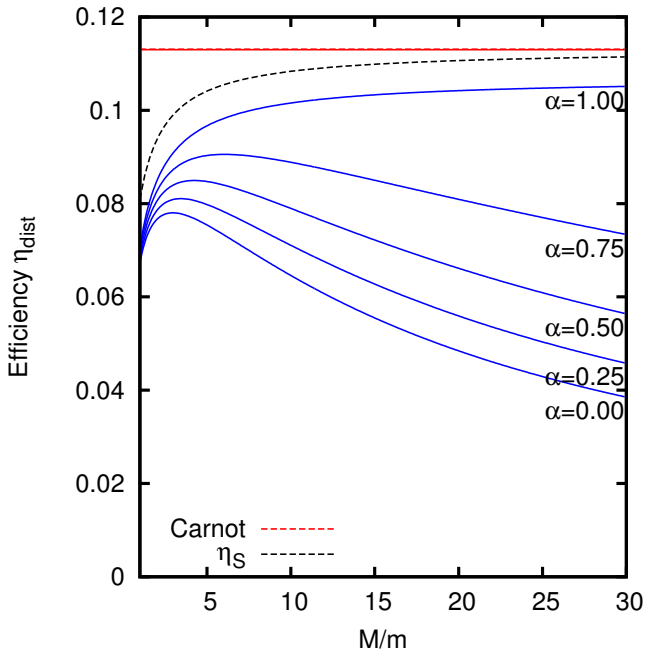

Figure 7: Efficiency of the distiller stage as a function of the ratio M/m between the concentrated solution and the pure solvent. The solute is NaOH with a concentration c_0=0.34 (molar fraction); T_L=30°C and T_H is the boiling temperature of the solution at concentration c_0. The various curves have been obtained with different values of the recovery factor α.

The expression of η_S of Eq. 11 suggests that it is possible to bring the efficiency η_{dist} closer to η_C by increasing M; actually this decreases the irreversible heat exchange of phase III by decreasing the difference between c_1 and c_0. This is confirmed by the graph in Fig. 7, which shows the dependence of η_{dist} on the ratio M/m.

However, as one can see from the graph, at high values of M/m, the values of η_{dist} start decreasing. This can be understood considering that the produced work is roughly proportional to m, and thus an increase of M/m leads to an increase of the total mass of solution per unit energy production; increasing the mass also increases the loss of heat due to the heat capacity in phase II, III and IV, that is not accounted for in η_S. Indeed, from Fig. 7, we can notice that increasing the recovery ratio α improves the efficiency.

The effect of the heat exchanges not accounted for by η_S, i.e. not connected to the vaporisation and condensation, can be easily written down in analytic form for $\alpha = 1$ and in the limit $M/m \to +\infty$, i.e. for $\eta_S = \eta_C$, although this condition is not physically feasible. By also considering λ and C as constant, we get:

$$\eta = \eta_C \frac{1 + \frac{T_H}{\tilde{T}} \left[1 - \left(\frac{1}{\eta_C} - 1 \right) \ln \frac{1}{1-\eta_C} \right]}{1 + \epsilon} \tag{12}$$

where $\tilde{T} = (C - C_s)/\lambda$ is a characteristic temperature, of the order of 1500 K for the water solutions we consider here, and $\epsilon = Cc_0/\lambda \partial T/\partial c$. Since $T_H << \tilde{T}$, the main contribution comes from ϵ: we see that the efficiency loss decreases as λ increases or C decreases.

The effect of the latent heat $\lambda(c)$ and of the specific heat $C(c)$ on the efficiency η_{dist} is shown in Fig. 8, where, for each value of the parameters, M/m is chosen at the maximum of η_{dist}. We see that the decrease of the specific heat $C(c)$ increases the efficiency; indeed it decreases the heat needed in phases II and IV. Its effect is similar to an increase of the heat recovery. We can also see an advantage in the increase of λ: since the produced work is roughly proportional to λm, an increase of λ leads to a decrease of the total mass processed per cycle, decreasing also the heat losses.

We have already shown that the main thermo-physical parameter determining the efficiency is the boiling point elevation. Now we also found a minor effect given by the increase of the latent heat of vaporisation and by a decrease of the specific heat capacity. The first two features (high boiling point elevation and latent heat of vaporisation) could appear surprising, since they are usually detrimental in distillation, the first because it imposes the use of higher temperatures for the evaporation, the second because it

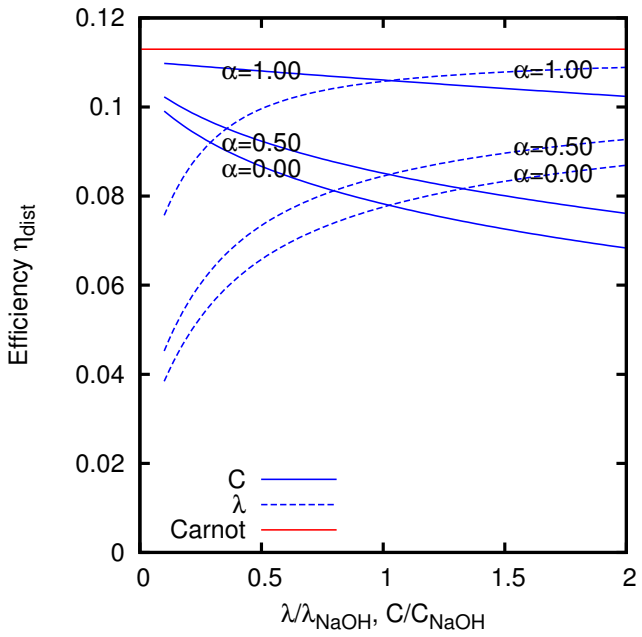

Figure 8: Efficiency of the distiller stage, as a function of the molar specific heat and of latent heat of vaporisation. The parameters are expressed as the ration with respect to the values they have for the NaOH solution with a concentration 0.34 (molar fraction). The various curves have been obtained with different values of the recovery factor α. The value of M/m is chosen in order to maximise the efficiency, i.e. at the peak shown in Fig. 7.

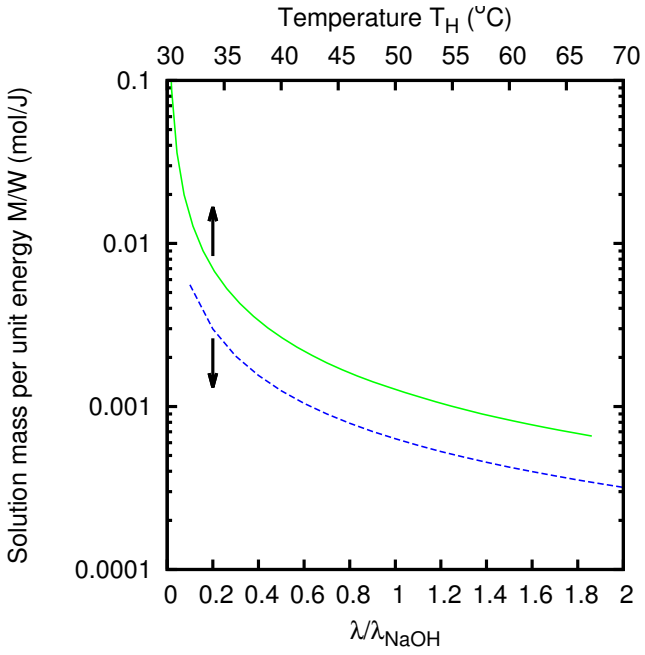

Figure 9: Mass per energy. Solution of NaOH with a concentration 0.34 (molar fraction). The various curves have been obtained with different values of the ratio M/m.

increases the required heat; however, this is due to the different goal of our HTCC, i.e. the production of energy rather than of distilled water.

The graph of Fig. 9 reports the mass of solution processed per cycle, at unit produced energy, as a function of the temperature T_H and as a function of λ, for various values of M/m. We see that the quantity of processed solution indeed decreases with the increase of temperature and with the increase of λ: this is the same that happens in distillation. However, this happens at fixed energy production: this means that the produced liquids have a higher density of mixing free energy when the temperature is higher or the latent heat of evaporation is larger

Indeed, a higher boiling point elevation is associated to a higher chemical potential of the solute. This is shown in Fig. 10, where the chemical potential (expressed in elettron-volts) is reported as a function of concentration. We see that the solutes with a higher boiling point elevation also have a higher chemical potential.

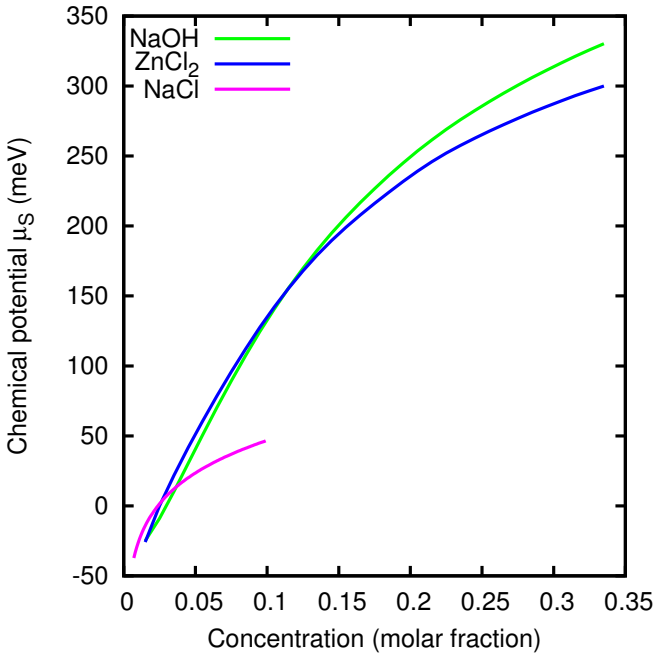

Figure 10: Chemical potentials of solute for aqueous solutions of NaOH, $ZnCl_2$ and NaCl at $T = 30°C$. The data stop at the molar fraction corresponding to the solubility of the salt. The quantities are known up to a constant and are thus arbitrarily displaced along the vertical axis.

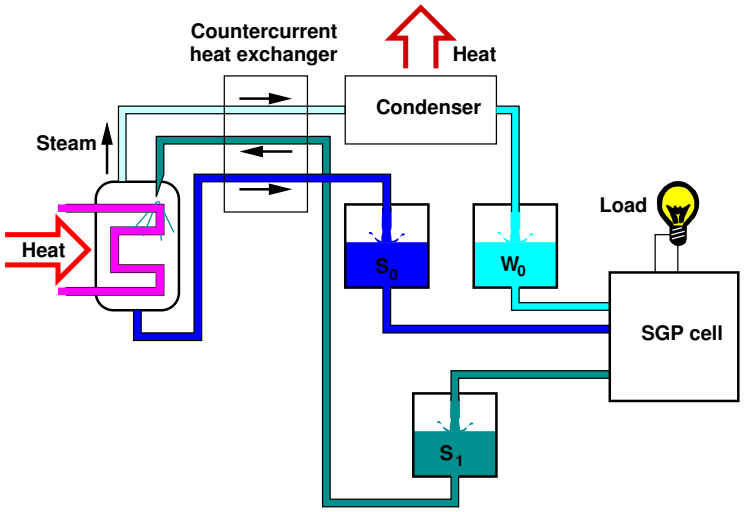

Figure 11: Practical realization of the HTCC with a continuous process.

It is worth noting that the calculation of the chemical potential can be easily performed from the value of ΔG, that, in turn, has been evaluated from teh thermo-physical parameters $C\,(c)$, $\lambda\,(c)$ and $T_{bp}\,(c)$, see SI Sect. 5.

4 Example of realization of the process

In Fig. 11, we show a practical scheme of the HTCC, with a single evaporator ("single effect"). At the working pressure, that is constant in all parts of the device, the concentrated solution and the pure solvent have respectively boiling temperatures T_H and T_L, with $T_H > T_L$ [9].

The SGP cell is fed with the concentrated solution S_0 and the distilled solvent W_0. The SGP cell generates a voltage, that is used for powering a load. The flow of current through the SGP cell induces the migration of the solute from the more concentrated to the less concentrated solution. The SGP cell is designed so that it consumes nearly completely the available concentration difference, while working in a continuous regime (see [12] for an example applied to RED technology), and gives as an output a completely mixed solution S_1.

The SGP cell works at a temperature slightly lower than T_L, in order to avoid that the pure solvent W_0 boils. The output solution S_1, at temperature T_L, is first sent to the countercurrent heat exchanger, where it receives heat; then it is sent to the evaporator, where additional heat is supplied,

until the temperature T_H is reached and part of the solvent evaporates. The concentrated solution S_0, at temperature T_H, is sent back through the countercurrent heat exchanger. If necessary, it is still further cooled, until the temperature T_L is reached, and finally comes back into the SGP cell.

The steam is condensed at temperature T_L, and the obtained distilled solvent is sent to the SGP cell. In principle, it is also possible to send also the steam through the countercurrent heat exchanger.

We assume that the flow of distilled solvent W_0, that is sent to the cell, is much smaller than the flow of the incoming solution S_0, so that the concentration of the outgoing solution S_1 is close to the concentration of S_0, and their boiling point is nearly the same.

Multiple effects are often used in order to increase the efficiency of distillation. They can be used also in our case. For example, a temperature difference of 100 K can be used for powering two effects for the distillation of $ZnCl_2$ solutions, each with 40 K of temperature difference; the evaporation in the second effect is obtained by the heat coming from the condensation of the vapour of the first effect. We can thus exploit with higher efficiency the available temperature difference. However, losses for the heat transfer also will increase.

Acknowledgements: We thank Pino Gherardi, Paolo Turroni (ET-EcoInnovative Technologies), Carlo Guidi, Francesco Gugole, Paolo Cesana and Duilio Calura (Italschell) for the collaboration in the development of the concept of the closed-cycle heat-to-current converter. We thank Luigi Galgani and Maarten Biesheuvel for useful discussions and suggestions on the manuscript.

References

[1] M. F. M. Bijmans, O. S. Burheim, M. Bryjak, A. Delgado, P. Hack, F. Mantegazza, S. Tennisson, and H. V. M. Hamelers. Capmix- deploying capacitors for salt gradient power extraction. *Energy Procedia*, 20:108–115, 2012.

[2] D. Brogioli. Extracting renewable energy from a salinity difference using a capacitor. *Phys. Rev. Lett.*, 103:058501, 2009.

[3] D. Brogioli, R. Zhao, and P. M. Biesheuvel. A prototype cell for extracting energy from a water salinity difference by means of double

layer expansion in nanoporous carbon electrodes. *Energ. Environ. Sci.*, 4:772–777, 2011.

[4] D. Brogioli, R. Ziano, R. A. Rica, D. Salerno, and F. Manteg azza. Capacitive mixing for the extraction of energy from salinity differences: survey of experimental results and electrochemical models. *J. Coll. Interf. Sci.*, 407:457–466, 2013.

[5] O. Burheim, B.B. Sales, O. Schaezle, F. Liu, and H. V. M. Hamelers. Auto generative capacitive mixing of sea and river water by the use of membranes. ASME 2011 International Mechanical Engineering Congress and Exposition (IMECE2011) (Denver, Colorado, USA) p. 483–492, paper no. IMECE2011-63459, 2011.

[6] A. Cipollina, A. Misseri, G. D'Alí Staiti, A. Galia, G. Micale, and O. Scialdone. Integrated production of fresh water, sea salt and magnesium from sea water. *Desalination and Water Treatment*, 49:390–403, 2012.

[7] R. H. Cole and J. S. Coles. *Physical principles of chemistry.* W. H. Freeman and Company, San Francisco, 1964.

[8] C. Ponce de León, A. Frías-Ferrer, J. González-García, D. A. Szánto, and F. C. Walsh. Redox flow cells for energy conversion. *J. Power Sources*, 160(1):716–732, 2006.

[9] E. Hala, J. Pickand V. Fried, and O. Vilim. *Vapour–liquid equilibrium.* Pergamon Press, 1967.

[10] Z. Jia, B. Wang, S. Song, and Y. Fan. A membrane-less na ion battery-based capmix cell for energy extraction using water salinity gradients. *RSC Adv.*, 3:26205–26209, 2013.

[11] N. D. Kaushika and K. S. Reddy. Performance of a low cost solar paraboloidal dish steam generating system. *Energ. Convers. Manag.*, 41(7):713–726, 2000.

[12] K. S. Kim, W. Ryoo, M. S. Chun, and G. Y. Chung. Simulation of enhanced power generation by reverse electrodialysis stack module in serial configuration. *Desalination*, 318:79–87, 2013.

[13] F. La Mantia, M. Pasta, H. D. Deshazer, B. E. Logan, and Y. Cui. Batteries for efficient energy extraction from a water salinity difference. *Nano Lett.*, 11:1810–1813, 2011.

[14] S. Loeb. Energy production at the dead sea by pressure-retarded osmosis: challenge or chimera? *Desalination*, 120(3):247–262, 1998.

[15] B. E. Logan and M. Elimelech. Membrane-based processes for sustainable power generation using water. *Nature*, 488(7411):313–319, 2012.

[16] M. Marino, L. Misuri, A. Carati, and D. Brogioli. Boosting the voltage of a salinity-gradient-power electrochemical cell by means of complex-forming solutions. *Appl. Phys. Lett.*, 105:033901, 2014.

[17] M. Marino, L. Misuri, A. Carati, and D. Brogioli. Proof-of-concept of a zinc-silver battery for the extraction of energy from a concentration difference. *Energies*, 7(6):3664–3683, 2014.

[18] R. L. McGinnis, J. R. McCutcheon, and M. Elimelech. A novel ammonia-carbon dioxide osmotic heat engine for power generation. *J. Membr. Sci.*, 305(1–2):13–19, 2007.

[19] A. Mclaren White. A derivation of Dühring's rule. *Ind. Eng. Chem.*, 22(3):230–232, 1930.

[20] J. Muschaweck, W. Spirkl, A. Timinger, N. Benz, M. Dorfler, M. Gut, and E. Kose. Optimized reflectors for non-tracking solar collectors with tubular absorbers. *Solar energy*, 68(2):151–159, 2000.

[21] R. W. Norman. Water salination: a source of energy. *Science*, 186:350–353, 1974.

[22] S. A. Omer and D. G. Infield. Design and thermal analysis of a two stage solar concentrator for combined heat and thermoelectric power generation. *Energ. Convers. Manag.*, 41(7):737–756, 2000.

[23] T. H. Pan, D. L. Xu, A. M. Li, S. S. Shieh, and S. S. Jang. Efficiency improvement of cogeneration system using statistical model. *Energ. Convers. Manag.*, 68:169–176, 2013.

[24] R. E. Pattle. Production of electric power by mixing fresh and salt water in the hydroelectric pile. *Nature*, 174:660, 1954.

[25] P. Peljo, D. Lloyd, D. Nguyet, M. Majaneva, and K. Kontturi. Towards a thermally regenerative all-copper redox flow battery. *Phys. Chem. Chem. Phys.*, 16:2831–2835, 2014.

[26] J. W. Post, H. V. M. Hamelers, and C. J. N. Buisman. Energy recovery from controlled mixing salt and fresh water with a reverse electrodialysis system. *Env. Sci. Techn.*, 42:5785–5790, 2008.

[27] J. W. Post, J. Veerman, H. V. M. Hamelers, G. J. W. Euverink, S. J. Metz, K. Nymeijer, and C. J. N. Buisman. Salinity-gradient power: Evaluation of pressure-retarded osmosis and reverse electrodialysis. *J. Membrane Sci.*, 288:218–230, 2007.

[28] T. I. Quickenden and Y. Mua. A review of power generation in aqueous thermogalvanic cells. *J. Electrochem. Soc.*, 142(11):3985–3994, 1995.

[29] R. A. Rica, R. Ziano, D. Salerno, F. Mantegazza, R. van Roij, and D. Brogioli. Capacitive mixing for harvesting the free energy of solutions at different concentrations. *Entropy*, 15(4):1388–1407, 2013.

[30] A. Rosato and S. Sibilio. Performance assessment of a micro-cogeneration system under realistic operating conditions. *Energ. Convers. Manag.*, 70:149–162, 2013.

[31] B. B. Sales, M. Saakes, J. W. Post, C. J. Buisman, P. M. Biesheuvel, and H. V. Hamelers. Direct power production from a water salinity difference in a membrane-modified supercapacitor flow cell. *Env. Sci. Techn.*, 44:5661, 2010.

[32] W. Spirkl, H. Ries, J. Muschaweck, and R. Winston. Nontracking solar concentrators. *Solar energy*, 62(2):113–120, 1998.

[33] I. Tlili, Y. Timoumi, and S. Ben Nasrallah. Analysis and design consideration of mean temperature differential stirling engine for solar application. *Renew. Energ.*, 33(8):1911–1921, 2008.

[34] M. Turek, B. Bandura, and P. Dydo. Power production from coal-mine brine utilizing reversed electrodialysis. *Desalination*, 221(1–3):462–466, 2008.

[35] J. N. Weinstein and F. B. Leitz. Electric power from differences in salinity: the dyalitic battery. *Science*, 191:557–559, 1976.

[36] F. Zhang, J. Liu, W. Yang, and B. E. Logan. A thermally regenerative ammonia-based battery for efficient harvesting of low-grade thermal energy as electrical power. SUBMITTED.